Published in final edited form as:
*Neuroimage*. 2009 April 15; 45(3): 656–661.

# Regional shape abnormalities in mild cognitive impairment and Alzheimer's disease

**Anqi Qiu**[*,a,b,c], **Christine Fennema-Notestine**[d,e], **Anders M. Dale**[e,f], **Michael I. Miller**[g,h,i], and **Alzheimer's Disease Neuroimaging Initiative**[1]

[a] Division of Bioengineering, National University of Singapore, Singapore

[b] Singapore Institute for Clinical Sciences, the Agency for Science, Technology and Research, Singapore

[c] Clinical Imaging Research Center, National University of Singapore, Singapore

[d] Department of Psychiatry, University of California, San Diego, La Jolla, CA, USA

[e] Department of Radiology, University of California, San Diego, La Jolla, CA, USA

[f] Department of Neurosciences, University of California, San Diego, La Jolla, CA, USA

[g] Center for Imaging Science, Johns Hopkins University, Baltimore, USA

[h] Institute for Computational Medicine, Johns Hopkins University, Baltimore, USA

[i] Department of Biomedical Engineering, Johns Hopkins University, Baltimore, USA

## Abstract

Magnetic resonance (MR) based shape analysis provides an opportunity to detect regional specificity of volumetric changes that may distinguish mild cognitive impairment (MCI) and Alzheimer's disease (AD) from healthy elderly controls (CON), and predict future conversion to AD. We assessed the surface deformation of seven structures (amygdala, hippocampus, thalamus, caudate, putamen, globus pallidus, body and temporal horn of the lateral ventricles) in 383 MRI volumes, based on data shared through the publicly available Alzheimer's Disease Neuroimaging Initiative (ADNI), to identify regionally-specific shape abnormalities in MCI and AD. Large deformation diffeomorphic metric mapping (LDDMM) was used to generate the shapes of seven structures based on template shapes injected into segmented subcortical volumes. LDDMM then constructed the surface deformation maps encoding the local shape variation of each subject relative to the template. Hierarchical models were developed to detect differences in local shape in MCI and AD relative to CON. Our findings revealed that surface inward-deformation in MCI and AD is most prominent in the anterior hippocampal segment and the basolateral complex of the amygdala. Most pronounced surface outward-deformation in MCI and AD occurs in the lateral ventricles. Mild surface inward-deformation in MCI and AD occurs in the anterior-lateral and ventral-lateral aspects of the thalamus,



* Corresponding author. Division of Bioengineering, National University of Singapore, 7 Engineering Drive 1, Block E3A #04-15, Singapore 117574. Fax: +65 6872 3069. bieqa@nus.edu.sg (A. Qiu)..

[1]**Data used in the preparation of this article were obtained from the Alzheimer's Disease Neuroimaging Initiative (ADNI) database (www.loni.ucla.edu/ADNI). As such, the investigators within the ADNI contributed to the design and implementation of ADNI and/or provided data but did not participate in analysis or writing of this report. A complete listing of ADNI investigators is available at http://www.loni.ucla.edu/ADNI/Data/ADNI_Authorship_List.pdf.

Conflicts of interest

Anders M. Dale is a founder and holds equity in CorTechs Labs, Inc, and also serves on the Scientific Advisory Board. The terms of this arrangement have been reviewed and approved by the University of California, San Diego in accordance with its conflict of interest policies.

with no evidence of regionally-specific deformation in the putamen or globus pallidus. Although the locations of the shape abnormalities in MCI and AD are primarily within the mesial temporal region, analyses support distinct components of correlated shape variation that may help predict future MCI conversion.

**Keywords**

Alzheimer's disease; Mild cognitive impairment; Deep structure shape; Diffeomorphic mapping

## Introduction

For almost a quarter of a century it has been clear that Alzheimer's disease (AD) will become a major public health burden. AD is a neurodegenerative disease that is the most frequent type of dementia in the elderly and affects almost half of all patients with dementia (Ferri et al., 2005). Advancing age is the primary risk factor for AD (Ferri et al., 2005). Mild cognitive impairment (MCI) has been considered as an intermediate cognitive state between healthy aging and dementia (Bennett et al., 2005). The relatively high annual conversion rate of 12% (range, 6% to 25%) from amnestic MCI to AD makes the MCI state scientifically interesting; only 1% to 2% of age-matched non-MCI subjects per year convert to AD (Mueller et al., 2005). Nevertheless, there remains considerable heterogeneity among MCI patients in clinical and pathological state, possibly because of the presence of the subjects within this group with preclinical forms of AD and other types of dementia, such as fronto-temporal dementia. Thus, more extensive characterization of MCI is needed to optimally distinguish MCI representing prodromal AD from those who will convert to another type of dementia, remain stable, or revert to normal cognitive status.

MR-based volumetric assessment of brain structures has been widely employed in the study of healthy aging, MCI, and dementia (Fox et al., 1996; Jack et al., 2002; Frisoni et al., 2005; Frisoni and Caroli, 2007). Consistent findings are volume loss in the hippocampus and entorhinal cortex (Jack et al., 1999; Dickerson et al., 2001; Frisoni et al., 2007; Fennema-Notestine et al., in press) and ventricular enlargement in both MCI and AD (Chetelat and Baron, 2003; Ridha et al., 2008; Fennema-Notestine et al., in press). Volumes of the amygdala, other structures in the medial temporal lobe (MTL) and the lateral temporal lobe also may be sensitive to MCI and prodromal AD although findings are conflicting (Visser et al., 1999; Convit et al., 2000; Fennema-Notestine et al., in press). Using brain warping techniques to characterize local shape variations may shed light on conflicting volumetric findings, and regional specificity of volumetric changes may represent *in vivo* findings shown in pathological studies. Previous structural shape studies in MCI and AD have only focused on individual structures, especially the hippocampus or lateral ventricles. The hippocampal regionally-specific shape effects were suggested to start in the subiculum and CA1, then propagate to CA2 and CA3 with disease progression (Apostolova et al., 2006; Wang et al., 2006). The enlargement in multiple areas of the lateral ventricles also has been reported recently (Ferrarini et al., 2006). Although regionally-specific shape analysis of the hippocampus or lateral ventricles has been demonstrated to be more powerful than volumetric analysis for predicting the locations of underlying pathology from normal aging, MCI to AD (Csernansky et al., 2005; Apostolova et al., 2006; Ferrarini et al., 2006; Qiu et al., 2008c), shape abnormalities in these regions may interact with surrounding structures. Thus, taking into account the shape variation of adjacent structures and identifying anatomical interrelationships among multiple structures may prove to be more sensitive in distinguishing MCI or AD from normal aging.

In this study, we employed data shared through the publicly available Alzheimer's Disease Neuroimaging Initiative (ADNI) database to assess shape abnormalities, relative to controls

(CON), for seven structures (body and temporal horn of the lateral ventricles, amygdala, hippocampus, thalamus, and three basal ganglia regions) in MCI and AD using the shape analysis pipeline developed under a large deformation diffeomorphic metric mapping (LDDMM) framework (Qiu and Miller, 2008). Unlike previous shape analysis on a single structure (Thompson et al., 2004; Ferrarini et al., 2006; Wang et al., 2006), our analysis took account of the shape deformations among the seven structures. Their covariance was used to identify shape abnormalities of these structures in MCI and AD. From our analysis, we expect to detect the involvement of hippocampal atrophy in regions near the subiculum and CA1–3 and the enlargement of the inferior lateral ventricle in MCI and AD as reported in previous neuroimaging studies (Csernansky et al., 2005; Apostolova et al., 2006; Ferrarini et al., 2006). In addition, we will explore shape abnormalities in nearby subcortical structures to examine the related effects across structures and expect to identify affected regions that are adjacent to and correlated with the hippocampal and ventricular abnormalities in MCI and AD.

## Methods

### Alzheimer's Disease Neuroimaging Initiative (ADNI)

Raw data were obtained from the ADNI database (http://www.loni.ucla.edu/ADNI). ADNI was launched in 2003 by the National Institute on Aging (NIA), the National Institute of Biomedical Imaging and Bioengineering (NIBIB), the Food and Drug Administration (FDA), private pharmaceutical companies and non-profit organizations. ADNI's goal is to test whether serial neuroimaging, biological markers, clinical and neuropsychological assessments can be combined to measure the progression of MCI and early AD. Determination of sensitive and specific markers of early AD progression is intended to aid researchers and clinicians to develop new treatments and monitor effectiveness, as well as lessen the time and cost of clinical trials.

ADNI is the result of efforts of many co-investigators from a broad range of academic institutions and private corporations. Subjects have been recruited from over 50 sites across U.S. and Canada. ADNI's goal was to recruit 800 adults, ages 55 to 90, to participate in the research (see www.adni-info.org).

### Participants

At the time of this study, 383 cases were available from the ADNI database and analyzed morphometrically at UCSD (Fennema-Notes-tine et al., in press)(Table 1). Briefly, subjects are 55–90 years of age, had an informant able to provide an independent evaluation of functioning, and spoke either English or Spanish (http://www.adniinfo.org/index.php?option=com_content&task=view&id=9&Itemid=43). All subjects were willing and able to undergo all test procedures including neuroimaging and agreed to longitudinal follow up. Specific psychoactive medications are excluded. General inclusion/ exclusion criteria are as follows:

1. Normal subjects: Mini-Mental State Examination (MMSE) (Folstein et al., 1975) scores between 24–30 (inclusive), a CDR of 0, non-depressed, non-MCI, and nondemented.
2. MCI subjects: MMSE scores between 24–30 (inclusive; exceptions made on a case by case basis), a memory complaint, objective memory loss measured by education adjusted scores on Wechsler Memory Scale Logical Memory II, a CDR of 0.5, absence of significant levels of impairment in other cognitive domains, essentially preserved activities of daily living, and an absence of dementia.
3. Mild AD: MMSE scores between 20–26 (inclusive; exceptions made on a case by case basis), CDR of 0.5 or 1.0, and meets NINCDS/ADRDA criteria for probable AD.

## Image protocol and volumetric segmentation

The present study employs LDDMM for shape analyses, as described in the next section, and this method relied on volumetric data created through a separate study (Fennema-Notestine et al., in press). These volumetric data were created from raw DICOM MRI scans downloaded from http://www.loni.ucla.edu/ADNI/Data/index.shtml, collected across a variety of scanners with protocols individualized for each scanner (http://www.loni.ucla.edu/ADNI/Research/Cores/index.shtml). These data were reviewed for quality, automatically corrected for spatial distortion due to gradient nonlinearity (Jovicich et al., 2006) and B1 field inhomogeneity, registered, and averaged to improve signal-to-noise. Volumetric segmentation based on FreeSurfer (Fischl et al., 2002) created volumes for the hippocampus, amygdala, caudate, putamen, thalamus, inferior lateral ventricle and body of the lateral ventricle for shape analyses (Fennema-Notestine, in press). Total intracranial volume (eTIV) (Buckner et al., 2004) was estimated to control for differences in head size.

## Data processing via LDDMM

LDDMM provides a set of template-based brain mapping algorithms dealing with images and surfaces (Vaillant et al., 2007; Qiu and Miller, 2008). Its resultant deformation map indexed over the template encodes the shape variation of subjects locally and can be used for detecting group difference in shapes. In our study, we designed a shape analysis pipeline as illustrated in Fig. 1 to assess shapes of the seven structures and identify anatomical abnormalities in disease. This pipeline aims to first delineate smooth volume and surface representations of the structures from MR images and then encode their surface deformations relative to a template using LDDMM.

**Template shape injection—**The original shapes of the subcortical structures were represented via a collection of homogeneous volumes with labels generated from FreeSurfer (Fischl et al., 2002). These labeled image volumes required preprocessing to improve smoothness of boundaries and to correct topological errors (e.g., undefined voxels in the volumes, or holes). This preprocessing reduced shape variation due to technical errors, and thus improved statistical power to detect shape abnormalities due to diseases. The preprocessing was performed with a template derived from a separate set of 41 manually-labeled volumes (Fig. 1) via a diffeomorphic template generation procedure (Qiu et al., 2008a). The template image was injected into FreeSurfer labeled images through a diffeomorphic transformation found by the LDDMM-image algorithm. The transformed template image is the “filtered” approximation of the parcellations for each individual subject. By the nature of the diffeomorphic map, such approximation represents the structures via a collection of homogeneous volumes with smooth boundary and correct topology. Their surface representation was created by composing the diffeomorphic map on the template surface.

**Surface deformation maps—**The LDDMM-surface mapping determines a scalar field indexed over the bounding surface of each structure to encode its shape variation relative to the template. We shall call this scalar field as “surface deformation map”, which is a log-Jacobian determinant of the deformation from the template to the surface of each subject. It indexes over the local coordinates of the template for statistical shape comparison across clinical populations. Its value represents the ratio of subject's structural volume to the template volume in the logarithmic scale: i.e. positive value corresponds to surface outward-deformation of subject's structure relative to the template at a particular location (red in panel 4 of Fig. 1), while negative value denotes surface inward-deformation of subject's structure relative to the template (blue in panel 4 of Fig. 1).

### Random field testing on shapes of multiple structures

To study anatomical interrelationships/correlations in the hippocampal–amygdala formation, subcortical regions, and ventricular systems, we developed a two-level hierarchical statistical analysis model by first building random fields within each structure based on its geometry and then modeling the interrelationship among these seven structures via principal component analysis (PCA).

In the first level, the deformation map, $\mu^i(x)$, of structure $i$ is assumed to arise from random processes modeled as random fields in the form of

$$\mu^i(\chi) \cong \sum_{k=1}^{N_i} F_k^i \psi_k^i(\chi), \quad \chi \in S^i_{\text{temp}}, \quad i \in \{\text{Am, Hp, Th, Cd, Pu, Pa, LV}\}, \tag{1}$$

where $\psi_k^i(x)$ is the $k^{th}$ basis function of the Laplace–Beltrami (LB) operator on the template surface, $S^i_{\text{temp}}.\psi_k^i(x)$ is deterministic and only dependent on the geometry of $S^i_{\text{temp}}$, which was detailed elsewhere (Qiu et al., 2006; 2008b; Qiu and Miller, 2008). The variation of $\mu^i(x)$ is thus represented through a finite number of LB-coefficients, $F_k^i, k=1, 2, \ldots, N_i$, where $N_i$ is determined based on the goodness fit at discrepancy level of 0.05, i.e., $\frac{|\mu^i(x)-\sum_{k=1}^{N_i} F_k^i \psi_k^i(x)|^2}{|\mu^i(x)|^2}=0.05$.

PCA was performed on the feature space of $F=\left[F_k^i, k=1, 2, \ldots, N_i, i \in \{\text{Am, Hp, Th, Cd, Pu, Pa, LV}\}\right]$, for modeling the shape correlation across the seven structures. $F$ is linearly projected to the orthogonal directions that carry the greatest shape variance. The lower-order PC-scores retain those characteristics of the shape variations in the subcortical regions. They are linearly independent variables. We thus test each of the PC-scores using a linear regression model with diagnosis (CON, MCI, AD) as independent variable after covarying for age, sex, and eTIV. Tukey post-hoc analysis was used to explore shape differences between any two groups. The anatomical interrelationship among the seven structures is determined by the pattern of the PCs with statistical significance.

To evaluate the reliability of statistical results conducted from the whole dataset, we divided our subjects into two subsets matched on age, sex and diagnosis ($n_1$ = 194; $n_2$ = 189). The above two-level hierarchical statistical analysis was repeatedly applied to each dataset.

## Results

We investigated shape abnormalities in MCI and AD through the surface deformation maps of the seven structures. Their deformation maps were characterized by total 120 LB basis functions using Eq. (1). PCA extracted 9 principal components that accounted for 85% of the variance in these LB-coefficients. Linear regression analysis revealed the 1st, 4th, and 7th PCs with significant effects of diagnosis at significance level of 0.005 ($p$-values in the first column of Table 2 after controlling for age, sex, and eTIV. Fig. 2 illustrates the scatterplot of these PC-scores within each diagnostic group.

Post-hoc pairwise comparisons revealed that the 1st and 7th PCs show significant group difference between CON and MCI; the 1st, 4th, and 7th PCs for the comparison between CON and AD; and only the 4th PC for the comparison between MCI and AD ($p$-values in Table 2). To visualize significant shape differences between any two groups, for instance, between CON

and MCI, we back projected the 1st and 7th PCs to the LB-coefficient space then to the template coordinates. Fig. 3 (a) illustrates this result in terms of ratio of local structural volume in CON to one in MCI. Based on the color scale, Fig. 3(a) suggests most pronounced surface inward-deformation in MCI in the anterior segment of the hippocampus, basolateral complex of the amygdala and mild surface inward-deformation in the anterior aspect of caudate nucleus, anterior-lateral and ventral-lateral aspects of the thalamus, and no regionally-specific effects on the putamen or globus pallidus. Fig. 3(a) also suggests most pronounced surface outward-deformation in the lateral ventricles and mild outward-deformation in the posterior segment of the hippocampus and medial aspect of the thalamus. Similarly, Figs. 3(b,c) show group shape differences between CON and AD constructed by PCs 1, 4, 7 and between MCI and AD constructed by the 4th PC, respectively. Interestingly, the atrophic regions of the amygdala and hippocampus are adjacent to the inferior lateral ventricle with the outward-deformation in the more severe disease group (Figs. 3(a–c)). To emphasize the significant changes in this mesial temporal area, Fig. 4 illustrates the significant group shape differences only in the hippocampus, amygdala and lateral ventricles.

The 4th PC contributes to the group shape differences between AD and CON or AD and MCI but not between CON and MCI (Table 2). We thus hypothesized that effects of AD on the seven shapes can be separated into two stages. The earlier stage associated with preclinical AD may be demonstrated by the 1st and 7th PCs; the late stage associated with AD by the 4th PC. To test this hypothesis, we respectively constructed the group differences between CON and AD using the 1st and 7th PC (Fig. 5(a)) and using the 4th PC (Fig. 5(b)). The pattern in Fig. 5 (a) is highly correlated to the group shape difference between CON and MCI in Fig. 3(a) (correlation coefficient: $r = 1$), while it has relatively low correlation with the one between MCI and AD in Fig. 3(c) ($r = 0.45$). In contrast, Fig. 5(b) is highly correlated with one in Fig. 3(c) ($r = 1$) but has low correlation with one in Fig. 3(a) ($r = 0.45$).

To evaluate the reliability of the findings shown in Fig. 3, the statistical testing procedure was repeatedly applied to the subset of the population. The results from the first subset are shown on the top row of Fig. 6, while those from the second subset are on the bottom row of Fig. 6. We quantitatively evaluated the correlation of the statistical surface deformation findings from the entire population (Fig. 3) with ones from the subsets (Fig. 6) in the pairwise group comparisons. All correlation coefficients are greater than 0.90 ($p$-values less than 0.0001), which suggest that the patterns of the differences in surface deformation obtained from the two subsets are highly consistent with those using the entire dataset.

## Discussion

To our knowledge, this is the first study to report on local shape differences of interrelated subcortical regions, hippocampal-amygdala formation, and lateral ventricles in MCI and AD relative to CON. Our analysis pipeline (Qiu and Miller, 2008) took the shape variations of the seven structures and identified their anatomical abnormalities in MCI and AD. We revealed that the mesial temporal region was most affected by MCI and AD, although changes were noted in additional regions. To be specific, the anterior segment of the hippocampus and the basolateral complex of the amygdala show more pronounced surface inward-deformation in MCI and AD when compared with CON. More pronounced surface outward-deformation occurs in the body and inferior lateral ventricles in MCI and AD. Our shape analysis also suggests a division of the AD-related effects on the shape abnormalities into two stages. The earlier stage corresponding to the MCI or prodromal AD is described by the 1st and 7th PCs; the later stage associated with mild AD is represented by the 4th PC. The correlation of the shape variation in each subject with these components may provide a way to identify MCI patients who have the shape abnormalities most like the one in AD and thus predict the

conversion of MCI to AD. Future longitudinal studies using our shape analysis pipeline are needed to examine the accuracy of this prediction.

Our findings of anterior hippocampal atrophy (near subiculum and CA1–3), often related to memory encoding (Lepage et al., 1998), and inferior lateral ventricular expansion in MCI and AD are in great agreement with previous neuroimaging findings (Apostolova et al., 2006; Ferrarini et al., 2006; Wang et al., 2006). As MCI and AD progress, the pattern and degree of differences in these structural shapes may be involved in a sequential order based on direct and indirect connections with the hippocampus. First, the basolateral amygdala and anterior hippocampus, which have significant interconnections, deform inwardly in MCI and AD. These findings are consistent with associated memory deficits in these populations, and correlative studies may help characterize this relationship further.

The anterior-lateral and ventral-lateral aspects of thalamus that connect primarily with the subicular complex of the hippocampus also show surface inward-deformation in MCI and AD. Furthermore, as additional projection zones of the subiculum and entorhinal cortex, the basal ganglia have no or mild shape changes in MCI and AD. These structures are less related to memory functions compared with the amygdala and hippocampus. Regionally-specific structural abnormalities in the amygdala and hippocampus could have widespread effects throughout their projection circuits as well as the cortex as AD progresses.

Areas with surface outward-deformation in the posterior hippocampus and medial thalamus may be related to partial voluming effects as the ventricular spaces expand adjacent to the hippocampus in these areas.

The present study focuses on the shapes around the subcortical regions in MCI and AD, and the addition of cortical regions also affected in these populations are of significant interest, such as the entorhinal cortex. Future integration of their shapes and thickness into our framework will provide a powerful system that characterizes structural abnormalities in MCI and early AD.

## Acknowledgments

This research was supported by grant (U24-RR021382) of the Morphometry Biomedical Informatics Research Network (BIRN, http://www.nbirn.net) funded by the National Center for Research Resources, National University of Singapore start-up grant R-397-000-058-133 (AQ), A*STAR SERC 082-101-0025 (AQ).

Data collection and sharing for this project was funded by the ADNI (PI: Michael Weiner; NIH grant U01-AG024904). ADNI is funded by the NIA, NIBIB, USFDA, and through contributions from: Pfizer Inc., Wyeth Research, Bristol-Myers Squibb, Eli Lilly and Company, GlaxoSmithKline, Merck & Co. Inc., AstraZeneca AB, Novartis Pharmaceuticals Corporation, Alzheimer's Association, Eisai Global Clinical Development, Elan Corporation plc, Forest Laboratories, and the Institute for the Study of Aging. Industry partnerships coordinated through the Foundation for NIH. The grantee organization is the Northern California Institute for Research and Education, and the study is coordinated by the Alzheimer's Disease Cooperative Study at the University of California, San Diego. ADNI data are disseminated by the Laboratory of Neuro Imaging at the University of California, Los Angeles.

## References

Apostolova LG, Dinov ID, Dutton RA, Hayashi KM, Toga AW, Cummings JL, Thompson PM. 3D comparison of hippocampal atrophy in amnestic mild cognitive impairment and Alzheimer's disease. Brain 2006;129:2867–2873. [PubMed: 17018552]

Bennett DA, Schneider JA, Bienias JL, Evans DA, Wilson RS. Mild cognitive impairment is related to Alzheimer disease pathology and cerebral infarctions. Neurology 2005;64:834–841. [PubMed: 15753419]

Buckner RL, Head D, Parker J, Fotenos AF, Marcus D, Morris JC, Snyder AZ. A unified approach for morphometric and functional data analysis in young, old, and demented adults using automated atlas-

based head size normalization: reliability and validation against manual measurement of total intracranial volume. NeuroImage 2004;23:724–738. [PubMed: 15488422]

Chetelat G, Baron JC. Early diagnosis of Alzheimer's disease: contribution of structural neuroimaging. NeuroImage 2003;18:525–541. [PubMed: 12595205]

Convit A, de Asis J, de Leon MJ, Tarshish CY, De Santi S, Rusinek H. Atrophy of the medial occipitotemporal, inferior, and middle temporal gyri in non-demented elderly predict decline to Alzheimer's disease. Neurobiol. Aging 2000;21:19–26. [PubMed: 10794844]

Csernansky JG, Wang L, Swank J, Miller JP, Gado M, McKeel D, Miller MI, Morris JC. Preclinical detection of Alzheimer's disease: hippocampal shape and volume predict dementia onset in the elderly. NeuroImage 2005;25:783–792. [PubMed: 15808979]

Dickerson BC, Goncharova I, Sullivan MP, Forchetti C, Wilson RS, Bennett DA, Beckett LA, deToledo-Morrell L. MRI-derived entorhinal and hippocampal atrophy in incipient and very mild Alzheimer's disease. Neurobiol, Aging 2001;22:747–754. [PubMed: 11705634]

Fennema-Notestine C, Hagler DJ Jr, McEvoy LK, Fleisher AS, Wu EH, Karow DS, Dale AM, the ADNI. Structural MRI biomarkers for preclinical and mild Alzheimer's Disease. Human Brain Mapping. in press.

Ferrarini L, Palm WM, Olofsen H, van Buchem MA, Reiber JH, Admiraal-Behloul F. Shape differences of the brain ventricles in Alzheimer's disease. NeuroImage 2006;32:1060–1069. [PubMed: 16839779]

Ferri CP, Prince M, Brayne C, Brodaty H, Fratiglioni L, Ganguli M, Hall K, Hasegawa K, Hendrie H, Huang Y, Jorm A, Mathers C, Menezes PR, Rimmer E, Scazufca M. Global prevalence of dementia: a Delphi consensus study. Lancet 2005;366:2112–2117. [PubMed: 16360788]

Fischl B, Salat DH, Busa E, Albert M, Dieterich M, Haselgrove C, van der Kouwe A, Killiany R, Kennedy D, Klaveness S, Montillo A, Makris N, Rosen B, Dale AM. Whole brain segmentation: automated labeling of neuroanatomical structures in the human brain. Neuron 2002;33:341–355. [PubMed: 11832223]

Folstein MF, Folstein SE, McHugh PR. Mini-mental state. A practical method for grading the cognitive state of patients for the clinician. J. Psychiatr. Res 1975;12:189–198. [PubMed: 1202204]

Fox NC, Warrington EK, Freeborough PA, Hartikainen P, Kennedy AM, Stevens JM, Rossor MN. Presymptomatic hippocampal atrophy in Alzheimer's disease. A longitudinal MRI study. Brain 1996;119(Pt 6):2001–2007. [PubMed: 9010004]

Frisoni GB, Caroli A. Neuroimaging outcomes for clinical trials. J. Nutr. Health Aging 2007;11:348–352. [PubMed: 17653497]

Frisoni GB, Testa C, Sabattoli F, Beltramello A, Soininen H, Laakso MP. Structural correlates of early and late onset Alzheimer's disease: voxel based morphometric study. J. Neurol. Neurosurg. Psychiatry 2005;76:112–114. [PubMed: 15608008]

Frisoni GB, Pievani M, Testa C, Sabattoli F, Bresciani L, Bonetti M, Beltramello A, Hayashi KM, Toga AW, Thompson PM. The topography of grey matter involvement in early and late onset Alzheimer's disease. Brain 2007;130:720–730. [PubMed: 17293358]

Jack CR Jr. Petersen RC, Xu YC, O'Brien PC, Smith GE, Ivnik RJ, Boeve BF, Waring SC, Tangalos EG, Kokmen E. Prediction of AD with MRI-based hippocampal volume in mild cognitive impairment. Neurology 1999;52:1397–1403. [PubMed: 10227624]

Jack CR Jr. Dickson DW, Parisi JE, Xu YC, Cha RH, O'Brien PC, Edland SD, Smith GE, Boeve BF, Tangalos EG, Kokmen E, Petersen RC. Antemortem MRI findings correlate with hippocampal neuropathology in typical aging and dementia. Neurology 2002;58:750–757. [PubMed: 11889239]

Jovicich J, Czanner S, Greve D, Haley E, van der Kouwe A, Gollub R, Kennedy D, Schmitt F, Brown G, Macfall J, Fischl B, Dale A. Reliability in multi-site structural MRI studies: effects of gradient non-linearity correction on phantom and human data. NeuroImage 2006;30:436–443. [PubMed: 16300968]

Lepage M, Habib R, Tulving E. Hippocampal PET activations of memory encoding and retrieval: the HIPER model. Hippocampus 1998;8:313–322. [PubMed: 9744418]

Mueller SG, Weiner MW, Thal LJ, Petersen RC, Jack CR, Jagust W, Trojanowski JQ, Toga AW, Beckett L. Ways toward an early diagnosis in Alzheimer's disease: the Alzheimer's Disease Neuroimaging Initiative (ADNI). Alzheimers Dement 2005;1:55–66. [PubMed: 17476317]

Qiu A, Miller MI. Multi-structure network shape analysis via normal surface momentum maps. NeuroImage 2008;42(4):1430–1438. [PubMed: 18675553]

Qiu A, Bitouk D, Miller MI. Smooth functional and structural maps on the neocortex via orthonormal bases of the Laplace–Beltrami operator. IEEE Trans. Med. Imaging 2006;25:1296–1306. [PubMed: 17024833]

Qiu A, Brown T, Fischl B, Kolasny A, Ma J, Buckner R, Miller MI. Subcortical structure template generation with its applications in shape analysis. NeuroImage. 2008a

Qiu A, Younes L, Miller MI. Intrinsic and extrinsic analysis in computational anatomy. NeuroImage 2008b;39:1803–1814. [PubMed: 18061481]

Qiu A, Younes L, Miller MI, Csernansky JG. Parallel transport in diffeomorphisms distinguishes the time-dependent pattern of hippocampal surface deformation due to healthy aging and the dementia of the Alzheimer's type. NeuroImage 2008c;40:68–76. [PubMed: 18249009]

Ridha BH, Anderson VM, Barnes J, Boyes RG, Price SL, Rossor MN, Whitwell JL, Jenkins L, Black RS, Grundman M, Fox NC. Volumetric MRI and cognitive measures in Alzheimer disease: comparison of markers of progression. J. Neurol 2008;255(4):567–574. [PubMed: 18274807]

Thompson PM, Hayashi KM, De Zubicaray GI, Janke AL, Rose SE, Semple J, Hong MS, Herman DH, Gravano D, Doddrell DM, Toga AW. Mapping hippocampal and ventricular change in Alzheimer disease. NeuroImage 2004;22:1754–1766. [PubMed: 15275931]

Vaillant M, Qiu A, Glaunes J, Miller MI. Diffeomorphic metric surface mapping in subregion of the superior temporal gyrus. NeuroImage 2007;34:1149–1159. [PubMed: 17185000]

Visser PJ, Scheltens P, Verhey FR, Schmand B, Launer LJ, Jolles J, Jonker C. Medial temporal lobe atrophy and memory dysfunction as predictors for dementia in subjects with mild cognitive impairment. J. Neurol 1999;246:477–485. [PubMed: 10431775]

Wang L, Miller JP, Gado MH, McKeel DW, Rothermich M, Miller MI, Morris JC, Csernansky JG. Abnormalities of hippocampal surface structure in very mild dementia of the Alzheimer type. NeuroImage 2006;30:52–60. [PubMed: 16243546]

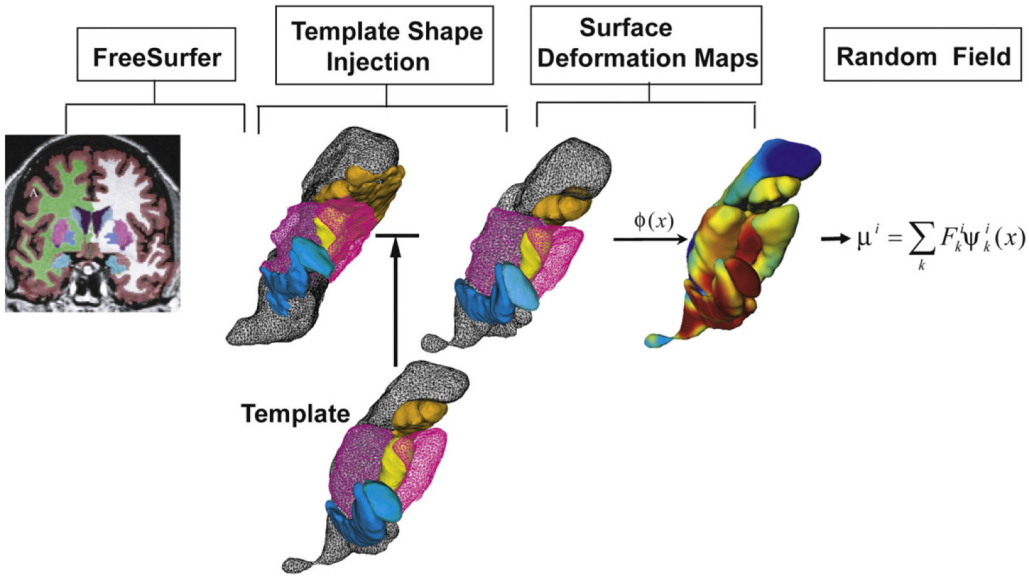


**Fig. 1.**

Figure illustrates the schematic of a shape analysis pipeline, including FreeSurfer subcortical segmentation, template shape injection, surface deformation map generation, and statistical random field testing. Panels 2 and 3 as well as template panel show color coded seven structures in the surface representation. The fourth panel illustrates the deformation map of one subject relative to the template, which is used in a random field model to make statistical inference.

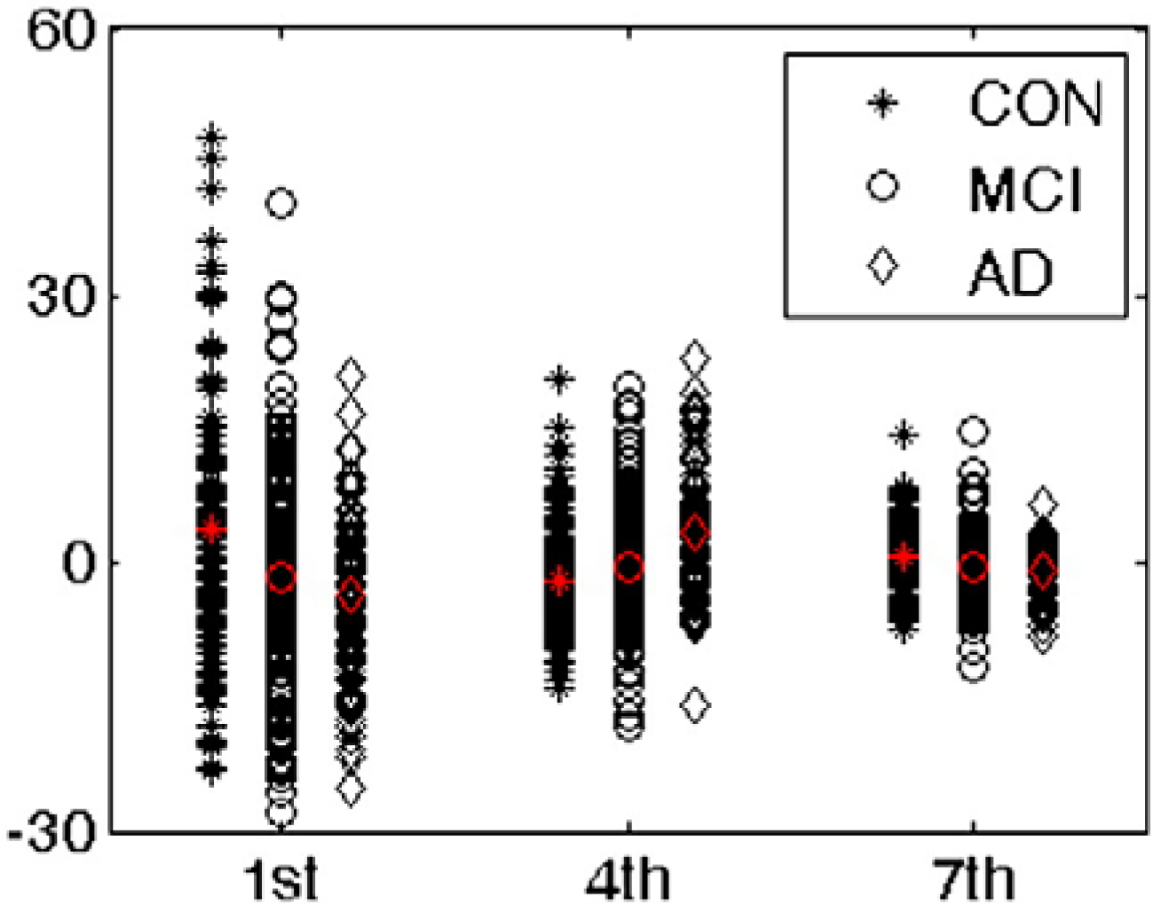


**Fig. 2.**
The 1st, 4th, and 7th PC-scores from each individual subject are shown. Asterisks, circles, and diamonds respectively represent the measurements from the groups of healthy controls, patients with MCI and AD. Red marks represent mean values. The p-values associated with group comparisons are listed in Table 2.

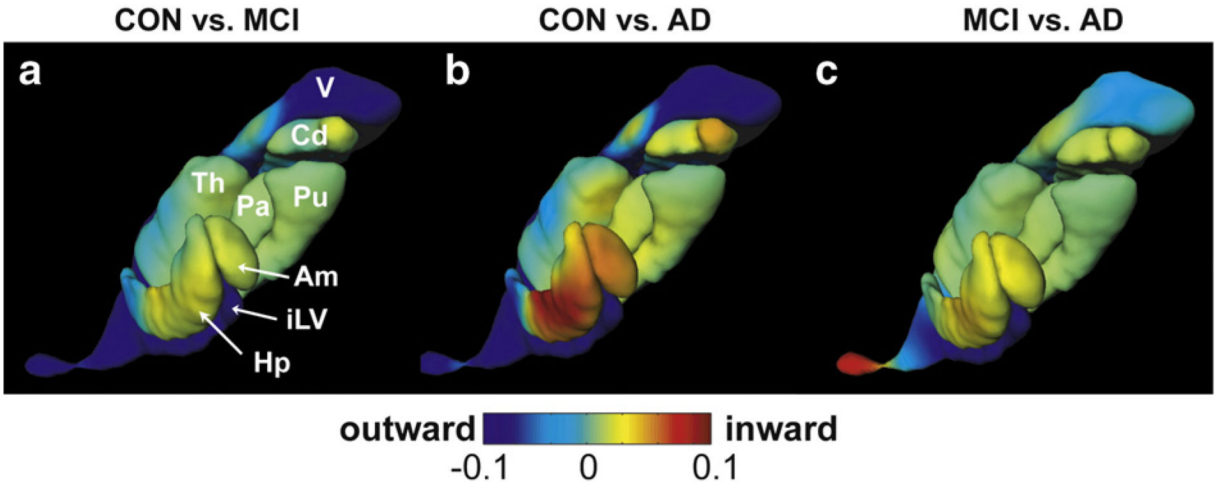


**Fig. 3.**

Panels (a–c) respectively show group differences in the surface deformation between CON and MCI, CON and AD, as well as MCI and AD. Warm color denotes regions where structures have surface inward-deformation in the latter group when compared with the former group. Cool color denotes regions where structures have surface outward-deformation in the latter group when compared with the former group. Key: Am — amygdala, Hp — hippocampus, V — ventricles, iLV — inferior lateral ventricles, Cd — caudate, Pu — putamen, Pa — globus pallidus, Th — thalamus.

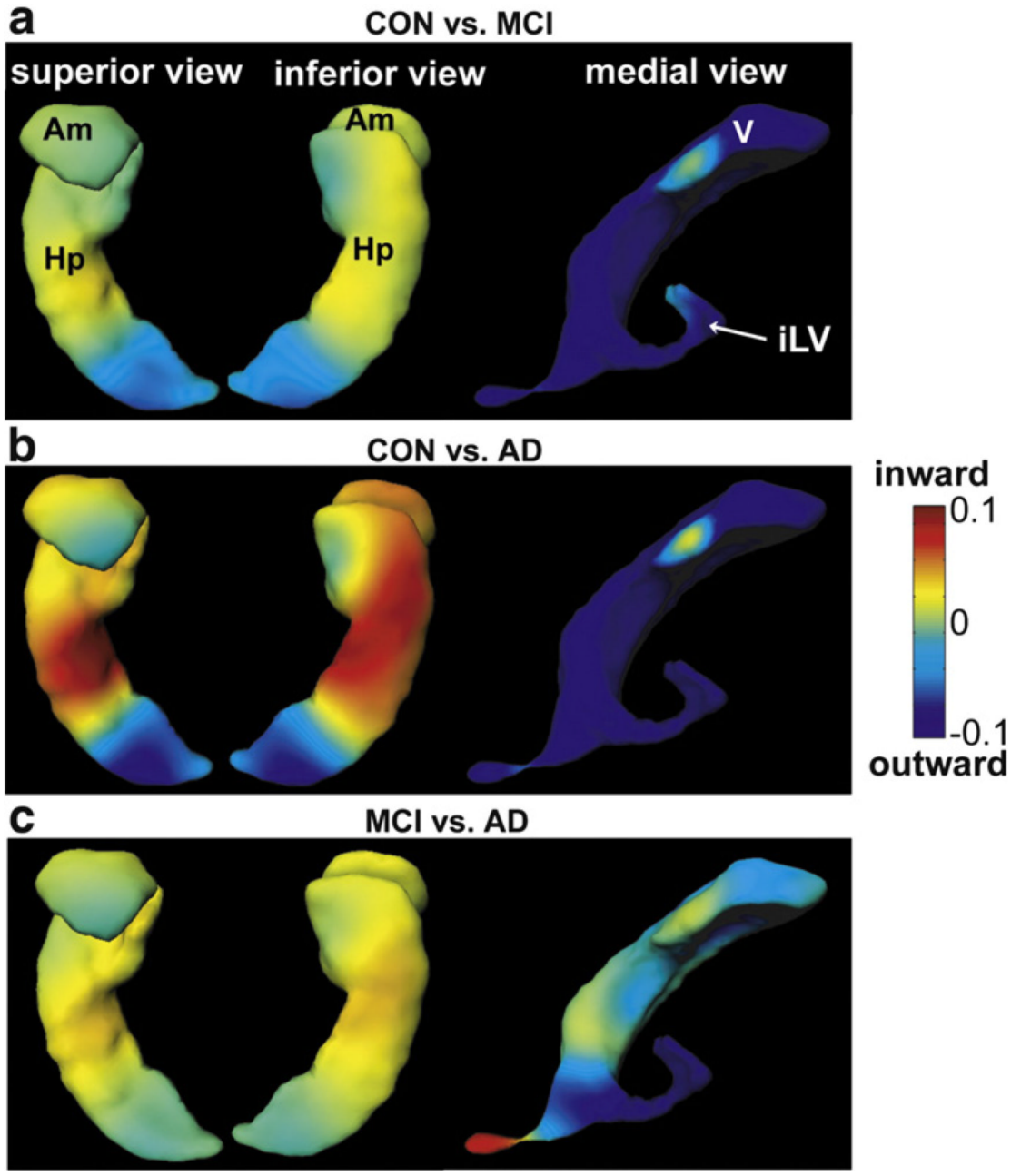


**Fig. 4.**

For visualization purpose, the deformation maps of the hippocampus, amygdala, and lateral ventricles shown in Fig. 3 are repeatedly illustrated in this figure. Panels (a–c) respectively show the deformation differences between CON and MCI, CON and AD, as well as MCI and AD. The superior and inferior views of the hippocampus and amygdala are shown in the first two columns and the medial view of the lateral ventricles is shown in the last column.

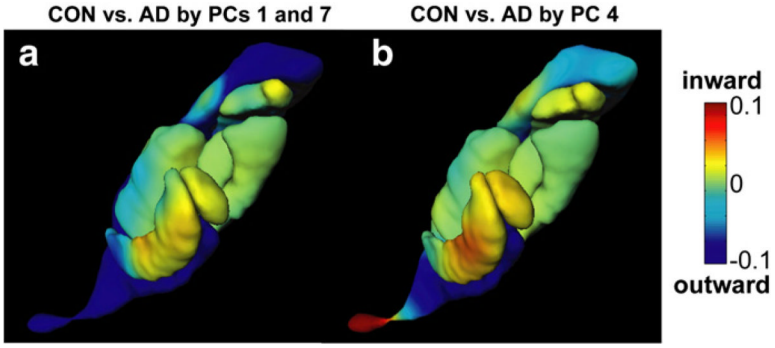


**Fig. 5.**

Panel (a) illustrates the shape difference between CON and AD constructed by the 1st and 7th PCs. Panel (b) illustrates the shape difference between CON and AD constructed by the 4th PC.

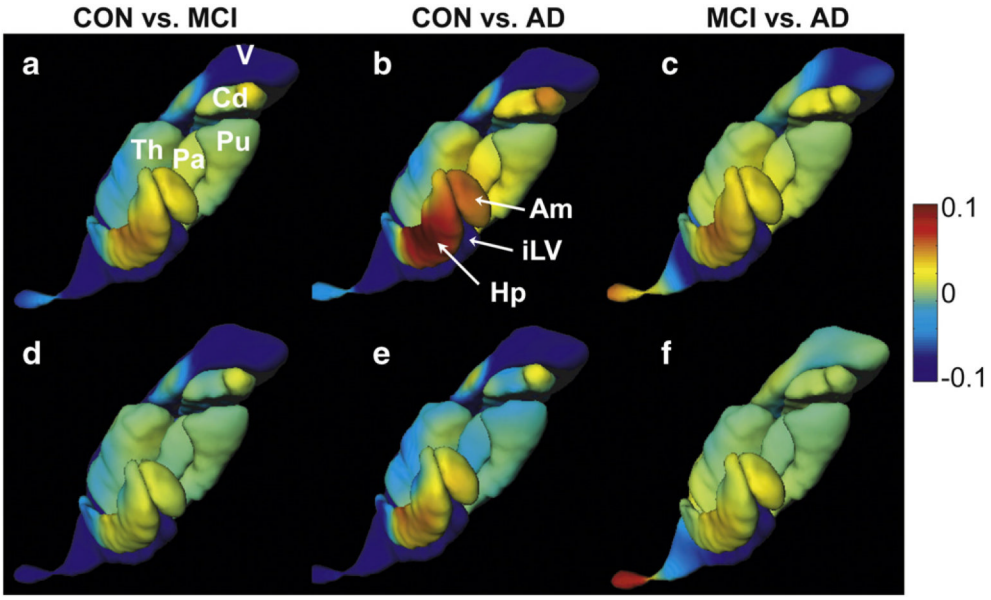


**Fig. 6.**

Reliability of the statistical findings. Panels (a–c) show the group comparisons in shapes conducted from the first subset with 194 subjects, while panels (d–f) illustrate those using the second subset with 189 subjects. The same color scale is used as in Figs. 3(a–c).

**Table 1**

Demographic information of 383 subjects

| Group | *N* | Sex (% male) | Age (mean±SD) | MMSE (mean±SD) | CDR (*n*) |
|---|---|---|---|---|---|
| CON | 133 | 53% | 75.8±4.9 | 29.1±1.0 | 0 (133) |
| MCI | 170 | 70% | 74.6±7.4 | 27.1±1.8 | 0.5 (170) |
| AD | 80 | 61% | 75.2±7.6 | 23.4±2.1 | 0.5 (38) 1.0 (42) |

Groups were not significantly different on age ($F$ =1.0, $p$>0.05). All groups differed on MMSE and CDR as expected based on diagnostic criteria (all $p$<0.001). Key: CON – healthy comparison subjects; MCI – mild cognitive impairment; AD – Alzheimer's disease; MMSE – Mini-Mental State Examination; CDR – Clinical Dementia Rating.

## Table 2

The first column lists the principal components (PCs) with significant diagnostic effects on the surface deformation, while the rest of the columns list the PCs associated with significant differences in the surface deformation between paired groups

| Diagnosis effect | CON vs MCI | CON vs AD | MCI vs AD |
|---|---|---|---|
| 1 (<0.0001) | 1 (0.0003) | 1 (<0.0001) | - |
| 4 (<0.0001) | - | 4 (<0.0001) | 4 (<0.0001) |
| 7 (0.0006) | 7 (0.0010) | 7 (0.0004) | - |

Their associated *p*-values obtained from linear regression are enclosed in parentheses. Key: CON vs MCI – shape comparison between the healthy comparison controls and patients with mild cognitive impairment; CON vs AD – shape comparison between the healthy comparison controls and patients with Alzheimer's disease; MCI vs AD – shape comparison between the patients with mild cognitive impairment and patients with Alzheimer's disease.